In Situ Transmission Electron Microscopy and Ion Irradiation of Ferritic Materials

MARQUIS A. KIRK,[1*] PETER M. BALDO,[1] AMELIA C.Y. LIU,[1] EDWARD A. RYAN,[1] ROBERT C. BIRTCHER,[1] ZHONGWEN YAO,[2] SEN XU,[2] MICHAEL L. JENKINS,[2] MERCEDES HERNANDEZ-MAYORAL,[3] DJAMEL KAOUMI,[4] AND ARTHUR T. MOTTA[4]

[1]*Electron Microscopy Center, Materials Science Division, Argonne National Laboratory, Argonne, Illinois 60439*
[2]*Department of Materials, University of Oxford, Oxford OX1 3PH, United Kingdom*
[3]*Division of Materials, CIEMAT, 28040 Madrid, Spain*
[4]*Department of Mechanical and Nuclear Engineering, Pennsylvania State University, University Park, Pennsylvania 16802*

KEY WORDS in-situ; ion-irradiation; ferritic alloys

ABSTRACT The intermediate voltage electron microscope-tandem user facility in the Electron Microscopy Center at Argonne National Laboratory is described. The primary purpose of this facility is electron microscopy with in situ ion irradiation at controlled sample temperatures. To illustrate its capabilities and advantages a few results of two outside user projects are presented. The motion of dislocation loops formed during ion irradiation is illustrated in video data that reveals a striking reduction of motion in Fe-8%Cr over that in pure Fe. The development of extended defect structure is then shown to depend on this motion and the influence of nearby surfaces in the transmission electron microscopy thin samples. In a second project, the damage microstructure is followed to high dose (200 dpa) in an oxide dispersion strengthened ferritic alloy at 500°C, and found to be qualitatively similar to that observed in the same alloy neutron irradiated at 420°C. *Microsc. Res. Tech. 00:000–000, 2009.*

INTRODUCTION

Candidate materials for structures in the next generation of fission reactors and first generation fusion power reactors include ferritic-martensitic steels with a typical composition Fe-9Cr-1Ti-1W and more complex mechanically alloyed oxide-dispersion strengthened (ODS) steels containing yttria nanoparticles. The attraction of these alloys for nuclear applications includes relatively low swelling under high-fluence neutron irradiation, reduced radiation embrittlement, good strength at relatively high temperatures, and low activation. However, a fundamental understanding of the radiation damage under high-fluence neutron irradiation, especially at elevated temperatures, is quite limited at present. Recently, these materials as well as more simple model ferritic alloys have become the subject of studies by transmission electron microscopy (TEM) with in situ ion irradiation over ranges of temperature and accumulated radiation damage equivalent in dpa (displacements per atom) to years of reactor exposure. The purpose of this article is to highlight some results from two ongoing research projects utilizing the in situ intermediate voltage electron microscope (IVEM)-Tandem Facility in the Electron Microscopy Center at Argonne National Laboratory.

The IVEM-Tandem Facility is a Department of Energy user facility which features the unique capability of high-quality conventional TEM during in situ ion irradiation at controlled sample temperatures. To study the microstructure evolution for advanced reactor applications, the IVEM-Tandem is extremely useful in that it can achieve high doses and allows following the kinetics of damage accumulation. Further technical details will be given in the next section and can be found at the website (www.msd.anl.gov/groups/ht). The Facility typically operates from 6 to 8 months out of the year serving about 15 groups mainly from universities, with about one third from outside the United States. Active research projects include irradiation studies on structural alloys for fission and fusion reactors, complex oxides for high-level nuclear waste storage, models for advanced nuclear fuels, implantation doping in semiconductors, and interplanetary dust.

IN SITU TEM-IRRADIATION FACILITY

The IVEM-Tandem Facility consists of an IVEM interfaced to either of two ion accelerators, an Implanter and a Tandem accelerator (Allen et al., 1996) (see Fig. 1), both by National Electrostatics Corp. The microscope is a Hitachi 9000 NAR with a side entry stage and with a slightly expanded objective pole piece gap of 11 mm to accommodate the beam line. It operates at voltages from 100 to 300 keV, with a point resolution of 0.25 nm at 300 keV (to work on ferritic samples, an electron energy of 200 keV is selected to produce a maximum atomic recoil energy well below the

Additional Supporting Information may be found in the online version of this article.

*Correspondence to: Mark Kirk, Electron Microscopy Center, Materials Science Division, Argonne National Laboratory, Argonne, IL 60439, USA. E-mail: kirk@anl.gov

Received 14 February 2008; accepted in revised form 7 July 2008

Contract grant sponsor: UChicago Argonne, LLC; Contract grant number: DE-AC02-06CH11357; Contract grant sponsors: US DOE Office of Science; UKAEA, Culham Science Centre; Nuclear Engineering Division at ANL; Pennsylvania State University.

DOI 10.1002/jemt.20670

Published online in Wiley InterScience (www.interscience.wiley.com).

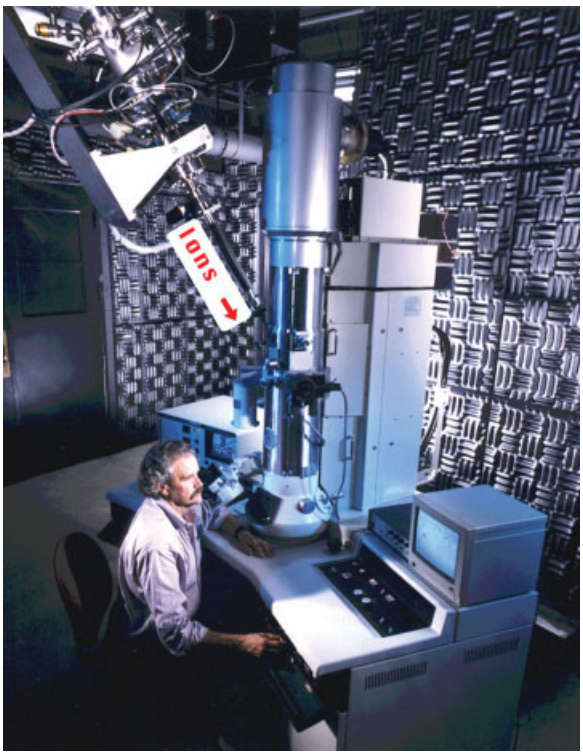

Fig. 1. IVEM-tandem in situ user facility: Hitachi 9000 NAR microscope, ion beam interface to microscope, and Dr. Charles W. Allen (responsible for installation and principal investigator, now retired). [Color figure can be viewed in the online issue, which is available at www.interscience. wiley.com.]

threshold for displacement). The turbo and ion-pumped vacuum system typically achieves 10^{-7} torr at the sample. This microscope has proven to be especially "user friendly," simple to operate, mechanically very stable during ion irradiation, and notably reliable. Data recording is provided by choices of film, a Gatan 622 video rate camera, and a Gatan Orius SC 1000 CCD camera with Digital Micrograph software. The introduction of a digital camera has provided a qualitative advantage in the effectiveness of our in situ experiments. It has permitted better and reproducible control of areas and diffraction conditions, and much more effective data acquisition and analysis during the progress of an experiment. Nobody misses the dark room.

The available ion beams range in mass from protons to Au, and in energy from 40 to 500 keV single-charged and 1 MeV double-charged for some ions. The ion-beam is raster scanned across an aperture in the ion beam line just before it enters the TEM column giving rise to a uniform irradiated area on the sample of a 2 mm diameter circle in the center of a standard 3 mm TEM specimen. The ion beam is incident at 30° from the microscope optic axis and electron beam, permitting continuous observation and data recording during irradiation under most sample tilting conditions that would be needed for bright and dark field imaging. The high angle of incidence of the ion beam is especially important in experiments on ferritic materials, when it is not feasible to tilt the specimen by more than about 20°. Ion dosimetry is achieved by catch (moveable) and skim Faraday cups within the microscope and 2 cm from the sample. Ion dose rates range up to 10^{16} ions cm^{-2} s^{-1} allowing, for example, damage levels up to 200 dpa (1 MeV Kr^{++}) to be reached in as little as a few hours.

A wide variety of Gatan sample holders are available for temperatures ranging from −258°C (15 K) to 1000°C (double tilting), a straining-heating holder (single tilt), and tilt-rotate holder with triple axis tilting. Energy dispersive X-ray spectroscopy is provided by an EDAX detector and Emispec controlling hardware and software.

Adjacent to the microscope room is a fume hood available for limited sample preparation and electropolishing. This has been especially useful for several of the experiments on pure Fe, low Cr alloys, and ODS ferritic alloys, which require a minimum of air exposure between preparation and insertion into the microscope. Occasionally, even mounting and insertion from within a nitrogen gas bag has been successful.

For a review of this and other TEM in situ irradiation facilities world-wide, see Birtcher et al. (2005).

HEAVY-ION IRRADIATIONS OF Fe AND Fe-Cr ALLOYS

The first of two projects to be highlighted here, led by M.L. Jenkins at the Department of Materials, University of Oxford, is designed to study the microstructural responses of pure Fe and Fe-Cr alloys to ion irradiation Yao et al. (in press), and Hernandez-Mayoral et al. (in press). In addition to the high damage rate, an advantage of using the IVEM-Tandem facility at ANL in this fundamental study has been unique dynamic observations of defect formation, mobilities, and interactions during irradiation. This has led to an understanding of how extended microstructures develop over a reactor lifetime.

One of the main results of the work by Yao et al. (in press) and Hernandez-Mayoral et al. (in press) is a comparison of radiation damage development in pure Fe and Fe with 5–11%Cr at several temperatures. These samples were irradiated using a self-ion beam (100–150 keV Fe ions) to avoid chemical implantation effects. A striking example of this comparison is shown in the associated video data (see Supporting Information) acquired during in situ ion irradiation at 300°C. A qualitative result is immediately obvious. Dislocation loops which probably formed initially in a cascade process have greater mobility in ultra-high purity (UHP) Fe, than in the Fe-8%Cr alloy. Further analysis by Yao et al. (in press) in UHP Fe samples finds that only loops with Burgers vectors, b = a/2 ⟨111⟩ are mobile. Loops with b = a ⟨100⟩ are present but are not mobile. Indirect evidence from an ex situ FIB (30 keV Ga) irradiation Yao et al. (in press) suggests that at least near-surface loops are vacancy in nature. Loop motion occurred primarily under ion irradiation, and would not have been detected without the in situ video observations. Loop motion was also noted to occur to lesser extent under electron (200 keV) irradiation/observation. The nature (interstitial or vacancy) of mobile loops could not be determined in the in situ experiments. Sample temperature increase under either or both the in situ

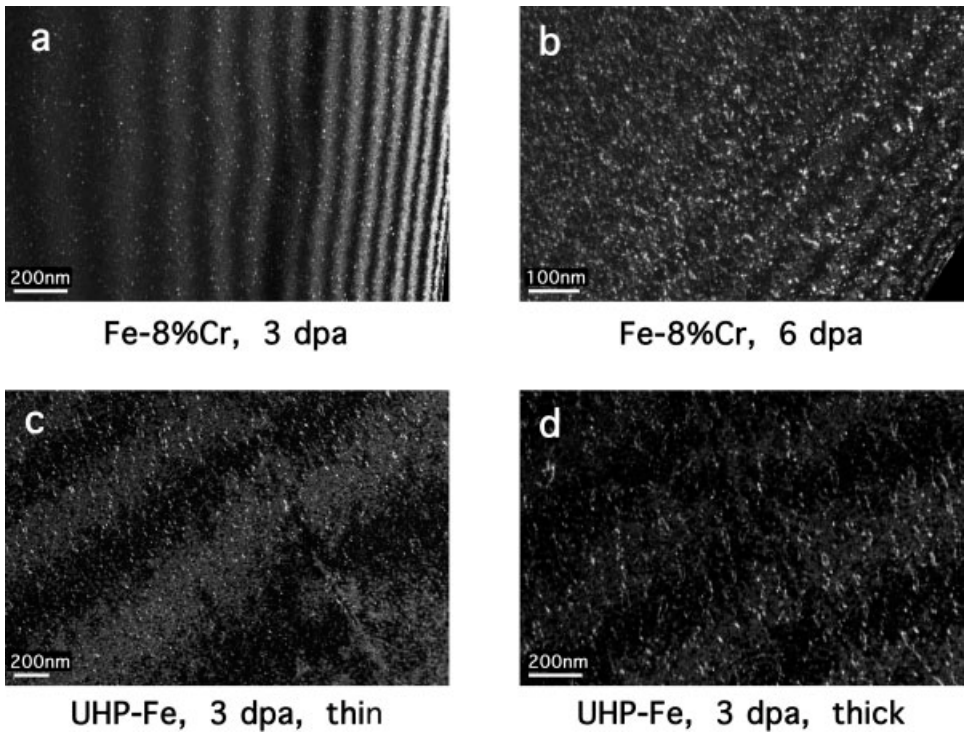

Fig. 2. Comparisons of defect microstructure in ultra-high purity (UHP) Fe and alloy of Fe with 8%Cr, irradiated with 150 keV Fe ions to given damage levels at a sample temperature 300°C. Imaging condition is weak-beam dark-field (WBDF) with $g = \langle 110 \rangle$ (g, $4g$).

ion and electron irradiations is insignificant (a few degrees at sample temperature of 300°C).

Two results of this difference in loop motion are suggested in Figure 2. Because of the reduced dislocation loop motion in the 8%Cr alloy, extended dislocation structures are less likely to form (compare panels a and b with panels c and d). Further, the loss of more mobile loops to a nearby surface is seen to produce a pronounced thickness effect in the UHP Fe experiment, but much less so in Fe-8%Cr. Approximate thicknesses vary from ~20 to 100 nm in Figure 2a, 20–40 nm in Figure 2c, and near 100 nm in Figure 2d. Note in Figure 2c that the loop density changes significantly from the thinnest area in the lower right corner to the thicker area at the upper left. Also the loops tend to form strings that are suggested by Yao et al. (in press) to result in the extended loops in thicker area of Figure 2d, which with further analysis are shown to be of interstitial nature. This, and other examples to be found in Yao et al. (in press), demonstrate how the necessary variation in thickness in most TEM samples can be used to advantage in understanding some fundamental aspects of irradiation defect formation and evolution with irradiation fluence.

Results closer to bulk irradiation are found in the ex situ work of Xu et al. (in press), examples of which are illustrated in Figure 3. Similar, but thicker, materials (pure Fe and Fe-8%Cr) were irradiated at 300°C with higher energy (1.5 MeV) Fe ions producing a damage peak (2.5 dpa) near 400–500 μm in depth. A time-controlled electropolishing technique (Yao et al., 2008) was employed to reveal the damage microstructure at this depth. Rather little difference in defect sizes and morphologies between the pure Fe and the Fe-8%Cr alloy is noted. However, the defect density in the Fe-8%Cr material may be somewhat higher, assuming comparable sample thicknesses.

A qualitative comparison at nearly the same dose and temperature of the thicker sample results in Figure 3 with the thinner sample results illustrated in Figure 2 is instructive. Although different irradiation energies are employed, rather similar defect densities and sizes are seen in both experiments, with the exception of the "thick" sample result in UHP Fe (Fig. 2d). In the Yao et al. (in press) experiment, a typical distance to nearest surface is 50 nm, whereas in the Xu et al. (in press) experiment the distance to the ion-beam entry surface is typically 500 nm. This order-of-magnitude difference apparently plays a role in the development of the more extended interstitial loops seen in Figure 2d. In this case the evolution of larger, elongated and roughly oriented loops may be a consequence of the influence of near surfaces, the thickness gradient, or thin film stresses during irradiation.

A limited comparison of loop geometries is possible between the Yao et al. (in press) (thin sample) and Xu et al. (in press) (thicker sample) experiments. Whereas, additions of Cr are shown in both experiments to roughly equalize the fraction of loops with Burgers vectors $a/2\ \langle 111 \rangle$ and $a\ \langle 100 \rangle$, a striking difference is found in pure Fe. In this case the ex situ bulk irradiation (2.5 dpa) experiment of Xu et al. (in press) found that 95% of loops have $b = a/2\ \langle 111 \rangle$, whereas the in situ thin foil experiment (irradiation to 1 dpa) of Yao et al. (in press) found 90% of loops have $b = a\ \langle 100 \rangle$. This is again a possible influence of nearby surface or thin-foil strain on loop geometry. Experiments to confirm this difference and to understand its origin are needed. However, in both experiments, the larger loops are determined to

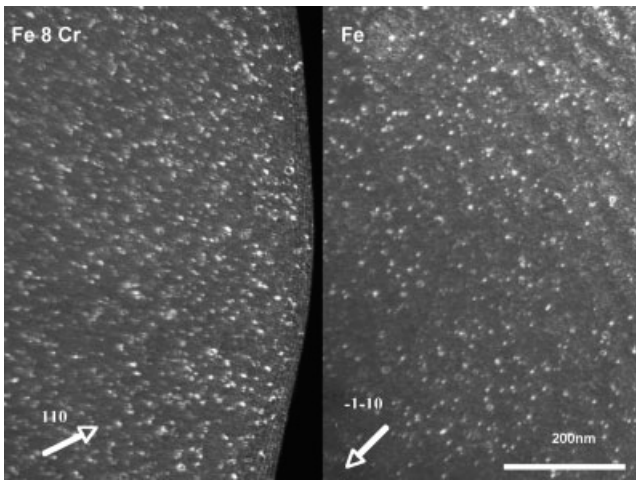

Fig. 3. Damage microstructures in bulk specimens of pure Fe and Fe-8%Cr following 1.5 MeV Fe ion irradiation at 300°C to 2.5 dpa and imaged in WBDF with $g = \langle 110 \rangle$.

be interstitial in nature, as revealed in an "inside-outside" measurement (Jenkins and Kirk, 2001).

HIGH-DOSE IRRADIATION OF ODS ALLOY

The maximum in situ irradiation level of damage with self ions is typically 10–20 dpa (about 2×10^{15} ions/cm^2) for a 1 day experiment in the IVEM-Tandem facility. To achieve higher levels of damage in a similar time requires heavier ion mass and high energies, typically 1 MeV Kr ions. The ion energy is designed such as to minimize implantation in the sample. About 1% of incident Kr ion dose is stopped in 100 nm sample thickness, but no evidence of Kr bubbles has been observed in numerous experiments. Additionally, sputtering at high doses from sample surfaces becomes a concern in the thinnest areas and can be estimated to be as much as 10 nm at 100 dpa. However direct observation of a thinning effect is not evident in these experiments. Under these conditions damage levels up to 200 dpa are thus reached in 1–2 day experiments, depending on the amount of microscopy performed at intermediate doses. An example of such high dose experiments is recent work led by Prof. A. Motta (Pennsylvania State University) on the IVEM-Tandem (Kaoumi et al., 2008) performed on an ODS ferritic steel MA957 alloy in situ at 500°C.

An example of the work of Kaoumi et al. (2008) is illustrated in Figure 4, which shows bright field micrographs taken during irradiation of the material MA957 (FE-14Cr-1Ti-0.3Mo-0.25Y2O3) with Kr ions to a dose of 200 dpa. Figure 4 includes an image (fourth panel) from the TEM work of Gelles (1996) on high-dose neutron irradiated MA957 at 420°C. In this figure, the areas shown at 0 dpa and 100 dpa are neighboring (but not identical), whereas the areas shown at 100 and 200 dpa are exactly the same, but at slightly different magnifications and tilts. A qualitative observation is that the grain structure, including sharp grain boundaries, is insensitive to this high level of damage in both the ion and neutron irradiations. Also, the dislocation networks that form within the grains show similar morphologies between the ion and neutron irradiations to high dose (200 dpa). This dislocation network appears substantially unchanged from 100 to 200 dpa in the in situ ion irradiation images. It should be pointed out that the sample tilts are slightly different and thus images of the defect structure vary between the different grains due to changes in diffraction condition with tilt. Another result (not shown) from the in situ experiment was that the structure of the large oxide particles was stable under this irradiation at 500°C. This suggests that the smaller oxide dispersion particles responsible for good alloy behavior were also stable.

In this same in situ irradiation experiment on the ODS alloy, quite small (1–2 nm) voids were probably revealed by through focus imaging, as shown in Figure 5. In comparison with the work of Gelles (1996), it can be noted that the void sizes in the ion irradiation to 200 dpa at 500°C are somewhat smaller than in the neutron irradiation to 200 dpa at 420°C (when the average void size was about 6 nm).

Finally, it is interesting to note that the in situ ion irradiation experiment required about 1 day, and the neutron irradiation required several years. The results summarized above suggest at least qualitatively that the damage microstructure is not very sensitive as one would expect for the different irradiation conditions and damage rates at these higher temperatures and in a material of small grain size with a high sink density of grain boundaries. The latter may also result in an insensitivity to the thin versus thick sample difference.

SUMMARY

The specifications of the IVEM-Tandem (EMC, ANL) in situ TEM-Irradiation facility have been outlined. To highlight some of the advantages of research at this facility, a few results from research projects of two user groups have been discussed.

Dislocation loop motion was recorded dynamically and displayed in an associated video (see Supporting Information) which revealed a striking effect of reduced motion in Fe-8%Cr compared with pure Fe during in situ ion irradiation. This difference in defect mobility results in differences in development of extended defect microstructures that are also influenced by sample thicknesses over a range from 20 to 500 nm. However, the use of TEM-thin sample can be useful in fundamental experiments to understand defect formation and interactions, especially if computer modeling can be employed in the future.

High damage levels, 200 dpa or end-of-reactor-lifetime, were employed to study microstructural changes at 500°C in an ODS ferritic alloy. Grain morphologies, dislocation networks, and void formation were compared qualitatively with a similar neutron irradiation experiment. In both in situ ion and ex situ neutron irradiations to 200 dpa, grain morphology and boundaries were stable and dislocation networks were similar. However, voids were slightly smaller in average size in the ion irradiation. The in situ high dose ion irradiation and TEM experiment required 1–2 days, whereas the ex situ neutron experiment required several years.

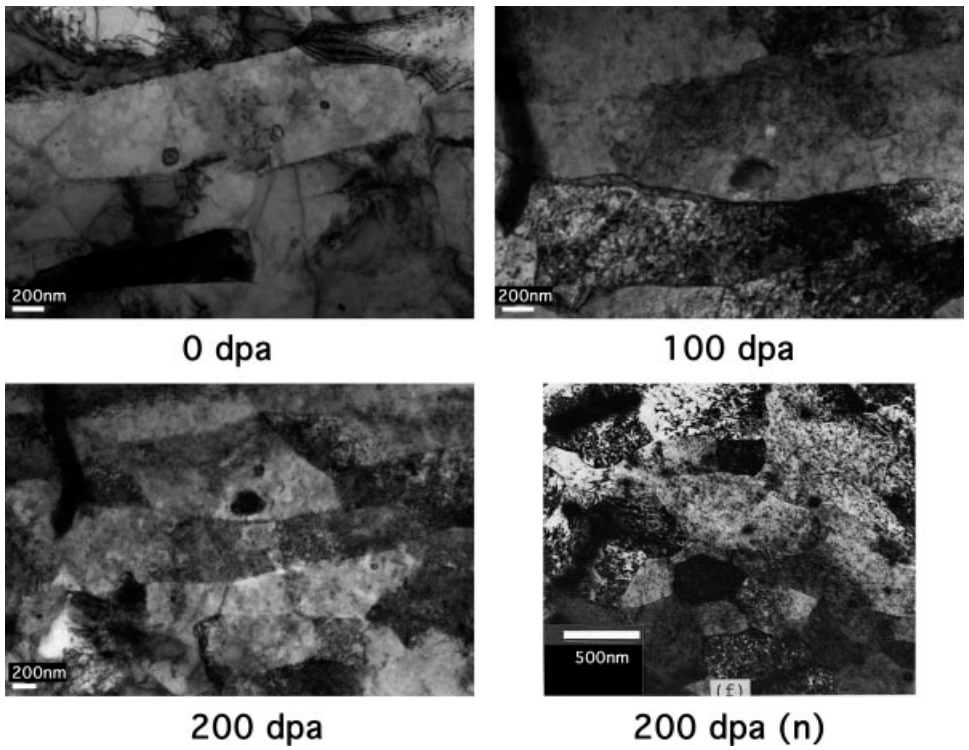

Fig. 4. Bright field images of MA957 ODS alloy irradiated in situ at 500°C with 1 MeV Kr^{++} ions (first three panels, size bar = 200 nm) and ex situ with fast neutrons at 420°C (Gelles, 1996, fourth panel, scale bar = 500 nm).

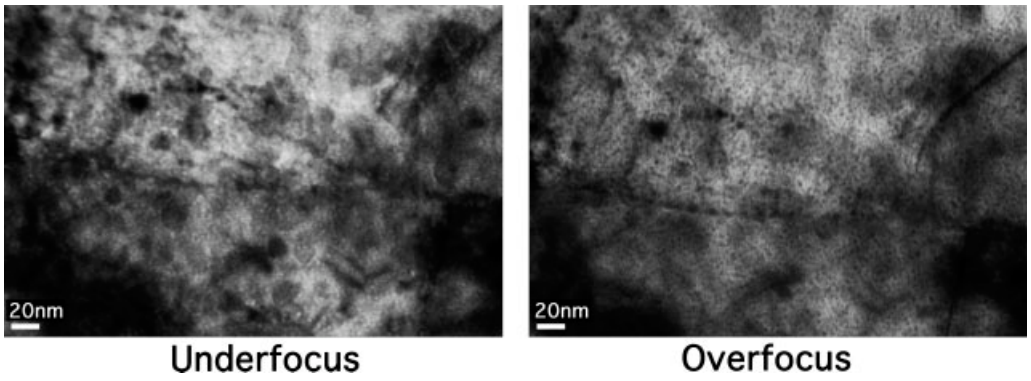

Fig. 5. Bright field defocus images of small (1–2 nm) voids in MA957 ODS alloy irradiated in situ at 500°C with 1 MeV Kr^{++} ions to a dose of 200 dpa. Scale bar = 20 nm.

ACKNOWLEDGMENTS

The authors thank Prof. J. Le Coze of the École de Mines de Saint Étienne for the provision of UHP iron, and Y. de Carian at CEA for the MA957 sample.

REFERENCES

Allen CW, Funk LL, Ryan EA. 1996. New instrumentation in Argonne's HVEM-tandem facility: Expanded capability for in situ beam studies. Mater Res Soc Symp Proc 396:641–646.

Birtcher RC, Kirk MA, Furuya K, Lumpkin GR, Ruault M-O. 2005. In situ transmission electron microscope investigations of radiation effects. J Mater Res 20:1654–1683.

Gelles DS. 1996. Microstructural examination of commercial ferritic alloys at 200 dpa. J Nucl Mater 233–237:293–298.

Hernandez-Mayoral M, Yao Z, Jenkins ML, and Kirk MA. 2008. Heavy-ion irradiations of Fe and Fe-Cr model alloys. Part 2: Damage evolution in thin foils at higher dose, Phil Mag, in press.

Jenkins ML, Kirk MA. 2001. Characterisation of radiation damage by transmission electron microscopy. Bristol: Institute of Physics Publishing.

Kaoumi D, Motta A, Kirk M. 2008. Characterization and in situ irradiation of MA957 ODS steel. In: American Nuclear Society Conference, Anaheim, CA.

Yao Z, Xu S, Jenkins ML, Kirk MA. 2008. Preparation of TEM samples of ferritic alloys. J Electron Microsc (Tokyo) 57:91–94.

Yao Z, Hernandez-Mayoral M, Jenkins ML, and Kirk MA 2008. Heavy-ion irradiations of Fe and Fe-Cr model alloys. Part 1: Damage evolution in thin-foils at lower doses, Phil Mag, in press.

Xu S, Yao Z, Jenkins ML. Heavy-ion irradiation damage in Fe-Cr alloys. J Nucl Mater, in press.